Journal of Pharmacology &Drug Development

eISSN: 2958-6801

OPEN ACCESS

Green Synthesis and Characterization of Gold Nanoparticles from Beta vulgaris L. and Their Cytotoxicity Against MDA-MB-231 and MCF-7 Cancer Cells

Abualfadhel Yahya [*,1], **Jenan Hussein Taha**[1] **Ibramim Abdullah Mahmood** [1]

1 Department of Physiology and Medical Physics, College of Medicine, Al-Nahrain University, Baghdad, Iraq
***Corresponding author:**
Received 23 Mar , Accepted 9 May , Published 1 Jun

ABSTRACT

With the increasing applications of gold nanoparticles in cancer treatment and medical delivery, it has become necessary to study the biological effects of gold nanoparticles. The study aimed to evaluate the biological effects of gold nanoparticles against the cancer cell.

Gold nanoparticles were characterized using several analytical techniques including X-ray Diffraction (XRD), Ultraviolet-Visible Spectroscopy (UV-VIS), Energy Dispersion X-ray (EDX), Atomic Force Microscopy (AFM), and Filed Emission Scanning Electron Microscopy (FE-SEM).. The characterization results confirmed the successful synthesis of high purity quasi-spherical gold nanoparticles with particle sizes ranging from 38 to 59 nm. The cytotoxic effect of the synthesized AuNPs was investigated using the Methyl Thiazolyl Tetrazolium (MTT) assay on both MCF-7 and MDA-MB-231 cell lines at six different concentrations. The results indicated a concentration-dependent inhibitory effect of gold nanoparticles on both cancer cell lines, with a high cytotoxic activity observed against the MDA-MB-231 cell line.

The results of this study indicate the potential use of gold nanoparticles against various types of cancer cell lines, as well as in treating cancerous diseases with in vivo cells.

Keywords : Nanoparticles, Gold Nanoparticles, Green Synthesis, Beta Vulgaris L, Breast Cancer, Cytotoxicity.

INTRODUCTION

Nanoparticles derive their name from the Greek word "nanos", meaning "dwarf". They are defined as minuscule particles with sizes that do not exceed 100 nanometres. These particles can be composed of a variety of materials, including carbon, organic compounds, metals, metal oxides, and others [1][2][3], Plants (green synthesis) and microorganisms (biosynthesis) play a role in the synthesis of nanoparticles. For instance, plant extracts and microorganisms that can reduce metal ions are used in the production of metal nanoparticles [4][5]. Beetroot is also used in the synthesis of metal nanoparticles because it contains chemicals (such as betalains[6], beta-cyanins[7], flavonoids[8], and tyrolites[9]) that contribute to the reduction of metal ions, specifically gold ions.[6]

Applications of gold nanoparticles have increased due to their exhibit stability in their metallic form at the nanoscale, unlike most other metal nanoparticles, due to the absence of oxide growth on their surface. [10][11]. Also, most of its properties change when it is at the nanoscale, depending on the method used to prepare the

nanoparticles[12]. In addition if the shape and size of the gold nanoparticles change, the Localized Surface Plasmon Resonance (LSPR) also changes, thus affecting the amount of absorption or scattering of incident light [13]. Gold nanoparticles possess a very high surface area and are non-toxic to normal biological processes, making them suitable for binding to various chemical and therapeutic agents. Their small size also facilitates their absorption by the target cells [14]. Not only have gold nanoparticles been used to deliver treatments, but they have also been used to deliver some vaccines. This is due to their controllable chemical and physical properties, which can be manipulated through various preparation methods and conditions, such as reducing crystal size or altering crystal structure[15]. Also when gold nanoparticles are linked to tumor necrosis factor-alpha (TNF-α is a cytokine protein produced by the immune system to defend the body and contributes to the engulfment of tumor cells), the protein's ability to engulf the tumor cells becomes greater. Raising the temperature also contributed to improving the effectiveness of this process.[16][17]. Cytotoxicity can be defined as the ability of a substance to disrupt the cell wall or destroy cells, leading to cell death through necrosis or programmed cell death. Gold nanoparticles (1-100 nm) exhibit cytotoxicity to both normal and abnormal cells due to their small size, making them suitable for numerous applications in pharmaceuticals [18]. Nanoparticles possess a high cytotoxicity against abnormal cells through several mechanisms, the most important of which is cellular oxidation, leading to programmed cell death (apoptosis).[19].

Therefore, this study aims to evaluate the cytotoxicity of gold nanoparticles synthesized by green synthesis against the cell lines MSF-7 and MDA-MB-231, and to study the structural, optical, and morphological properties of the gold nanoparticles synthesized by green synthesis.

Material and Method

Preparation of Plant Extract

Beetroot was purchased from local markets and soaked in deionized water to remove all soil and impurities. After one hour, the outer crust of the beetroot was peeled with a sharp knife, and they were soaked again in deionized water to ensure they were completely free of any remaining soil and impurities. The beetroot was then boiled in deionized water for two hours. Finally, they were placed in a medical gauze pad to be squeezed to extracted their active ingredients. Until obtain 200 ml of beetroot extract [20].

Preparation of Gold Nanoparticles

Gram of uric acid [〖HAuCl〗_4.3(H_2 o)] was dissolved in 100 ml of deionized water (pH = 3), and to raise the pH and make it alkaline, drops of sodium hydroxide (NaOH) (we dissolved a gram sodium hydroxide in one liter of deionized water and then added as dropped approximately six milliliters on uric acid) were added to achieve a pH of 8. A 50 ml of uric acid [〖HAuCl〗_4.3(H_2 o)] (pH = 8) was added to 200 ml of the beetroot extract and stored for 6 hours in a refrigerator at 4 °C, to prevents degradation of active compounds, reduces microbial growth, and Maintains consistent reaction behavior. After this time, the solution was centrifuged at 8000 rpm for half an hour, and the precipitate was washed with deionized water (this process was repeated five times). After washing, the solution was dried in a thermal oven at 80 °C for 6 hours, and the dried precipitate was re-incinerated in a high-temperature oven at 550 ℃ for 2 hours to obtain a highly crystalline powder and remove most of the organic materials used in the preparation method.

Methyl Thiazolyl Tetrazolium (MTT) assay

Culture on a Cytotoxicity Plate

To uprooting cancer cells from the wall of a cell culture flask(T-flask), empty the cell culture flask(T-flask) of complete medium and spray 1 ml of "Trypsin" solution onto the flask wall to help uprooting the cells from the wall. Store the flask in an autoclave for 8 to 10 minutes. After examining the flask under a light microscope, we will observe that the cells are floating in the "Trypsin" solution, indicating that the cancer cells have been effectively uprooting from the wall. Next, add 6 ml of complete medium to the cell culture flask(T-flask) for culture on a cytotoxicity plate. Using a pipette, 150 µL of cell culture with complete medium into each hole in the plate. Store the cytotoxicity plate in an autoclave for 24 hours at 37°C.

Dissolve Nanoparticles with Cancer Cells

10 milligrams of nanoparticles were re-dissolved in 50 microliters of dimethyl sulfoxide (DMSO) solution[21]. The re-dissolved nanoparticle solution was then diluted with 4 milliliters of complete medium solution to obtain a 100% concentration, this is the first concentration. Next, 5 milligrams of nanoparticles were weighed and dissolved in 10 microliters of DMSO solution, then diluted with 2 milliliters of complete medium solution. Following this, 2.5 milligrams of nanoparticles were weighed and dissolved in 5 microliters of DMSO solution, then diluted with 1 milliliters of complete medium solution. Finally, 1.25 milligrams, 0.625 milligrams, 0.3125 milliliters, and 1.6 milligrams of nanoparticles were weighed, and the same concentrations of DMSO solution and complete medium solution were repeated [21]. This resulted in six different concentrations of nanoparticles. Then, using a pipette, we take 100 microliters of each concentration into 6 holes of the cytotoxicity test plate in an autoclave for 24 hours at a temperature of 37°C (Figure 1).

Figure 1: Preparation of 96-well microplate by multichannel pipetting of gold nanoparticle dilutions for MTT cytotoxicity assay against MCF-7 and MDA-MB-231 cancer cell lines.

Toxicity Assay Investigation

On the final day, 10 microliters of "Methyl Thiazolyl Tetrazolium" (MTT) dye are take in each well of the cytotoxicity plate and Store in an autoclave at 37°C for 2 to 4 hours until a color change is observed in each well. The plate is then analyzed using ELISA to determine the lethality at each concentration as well as by using equation (2-1).

$$\text{Inhibition Rate} = \frac{\text{Control} - \text{Concentrition Inhibtion}}{\text{Control}} \times 100\% \text{ -------- } (2\text{-}1)$$

RESULT

X-Ray Diffraction for Gold Nanoparticles (AuNPs)

The XRD of gold nanoparticle, prepared using the beetroot extract, show clear diffractions that indicate the formation of gold NPs with a relatively pure crystalline phase with a centered cube structure (FCC), where the highest peak appears at an angle. $2\Theta \approx 38.1°$ and attributed to the crystalline level (111), which is the preferred trend for the growth of nanoparticles, as commonly in green methods. Additional peaks appear at the corners $2\theta \approx 44.3°$, 64.5°, and 77.5°, which date back to the crystalline levels (200), (220). and (311), respectively. As demonstrated in Table 1 and Figure 2. In addition to the main peaks, weak secondary peaks are observed at relatively low angles such as 28°, 31°, and 34°, as well as other small peaks of limited intensity. The crystalline size and micro-stress of gold nanoparticles prepared using beetroot extract were estimated based on X-ray diffraction peak analysis and by applying the Debye-Scherer equation, and as illustrated in table.

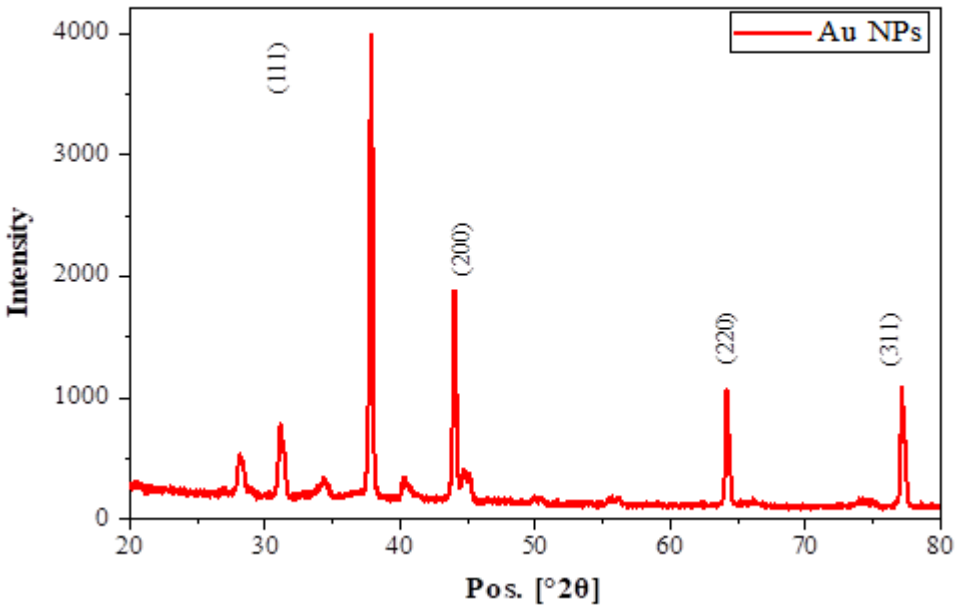

Figure 2: XRD Pattern of AuNPs Powder Extracted from Beetroot Plant

Table 1: Identification Parameters of Au NPs Obtained from XRD Results

Pos. [°2θ]	FWHM [°2θ]	Crystallite Size [nm]	Micro Strain [%]
37.8054	0.2197	45.4	0.26203
44.7193	0.471	12.3	0.82354
64.161	0.206	54.5	0.13301
77.1329	0.2102	58.4	0.10573

Ultra Vault – Visible Spectrum (UV-Vis Spectrum) for Gold Nanoparticles (AuNPs)

The UV-Vis absorption spectrum of gold nanoparticles prepared using the green synthesis method exhibits distinctive optical behavior, reflecting the successful bioreduction of gold ions and nanoparticle formation. A significant increase in absorption is observed in the UV region at shorter wavelengths, and a broad peak is present in the near-visible region, without the sharp, well-defined plasmonic peak typically expected for gold nanoparticles near 520–530 nm.as shown in Figure 3 a.

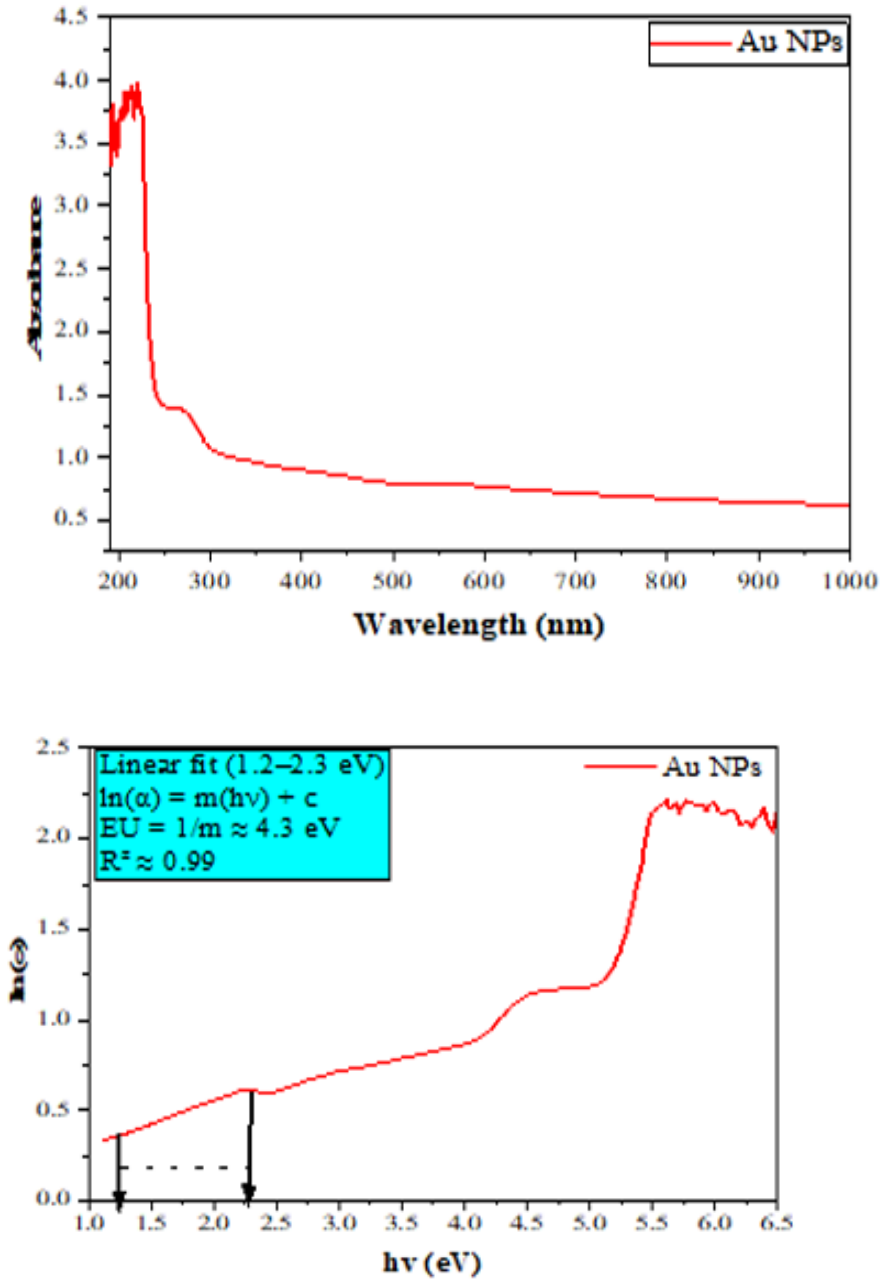

Figure 3: (a) Absorption Spectra of AuNPs Powder Extracted from Beetroot Plant, and (b) Urbach Energy of AuNPs Powder Extracted from Beetroot Plant

To quantitatively characterize this optical disturbance, the low-energy absorption tail was analyzed using the ln(α) representation versus the photon energy hν. The resulting curve showed a distinct linear region, which was used to extract the Urbach EU value. The EU value was approximately 4.3 eV, indicating a high degree of electronic disturbance and surface scattering associated with the small particle size and its strong interaction with the bio-medium used in the preparation As in Figure 3b.

Field Emission-Scanning Electron Microscopy (FE-SEM) for Gold Nanoparticles (AuNPs)

The Field Emission Scanning Electron Microscopy (FE-SEM) image of gold nanoparticles prepared using beetroot extract via green synthesis reveals a distinctive morphological structure consisting of closely packed, quasi-spherical nanoparticles with clear micro-clumping and a relatively heterogeneous size distribution. Measurements shown in the image indicate that the particle diameters fall within the nanoscale, with approximate values ranging from approximately 38 to 59 nm, and some larger clusters appearing due to the aggregation of several primary particles as illustrated in the Figure 4.

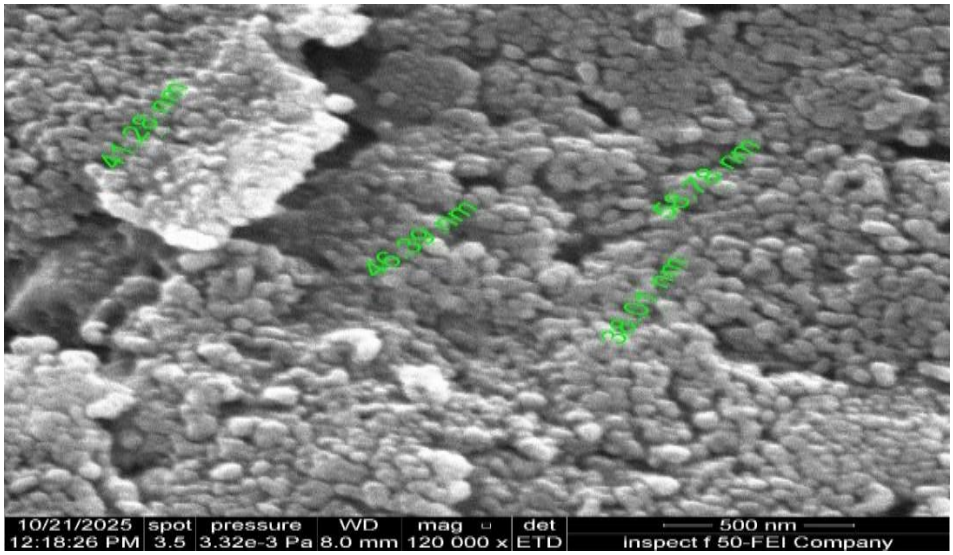

Figure 4: FE-SEM image for Gold Nanoparticles (AuNPs)

Energy Dispersive X-Ray (EDX) for Gold Nanoparticles (AuNPs)

Energy-dispersive X-ray spectroscopy (EDS) analysis of gold nanoparticles prepared using beetroot extract shows the appearance of strong, characteristic peaks belonging to the element gold (Au), particularly at energies approaching ~2.1 keV (Au–M) and also at higher energies attributed to Au–L transitions. Weak peaks belonging to elements such as C, O, Na and Cl were observed this is shown in Figure 5.

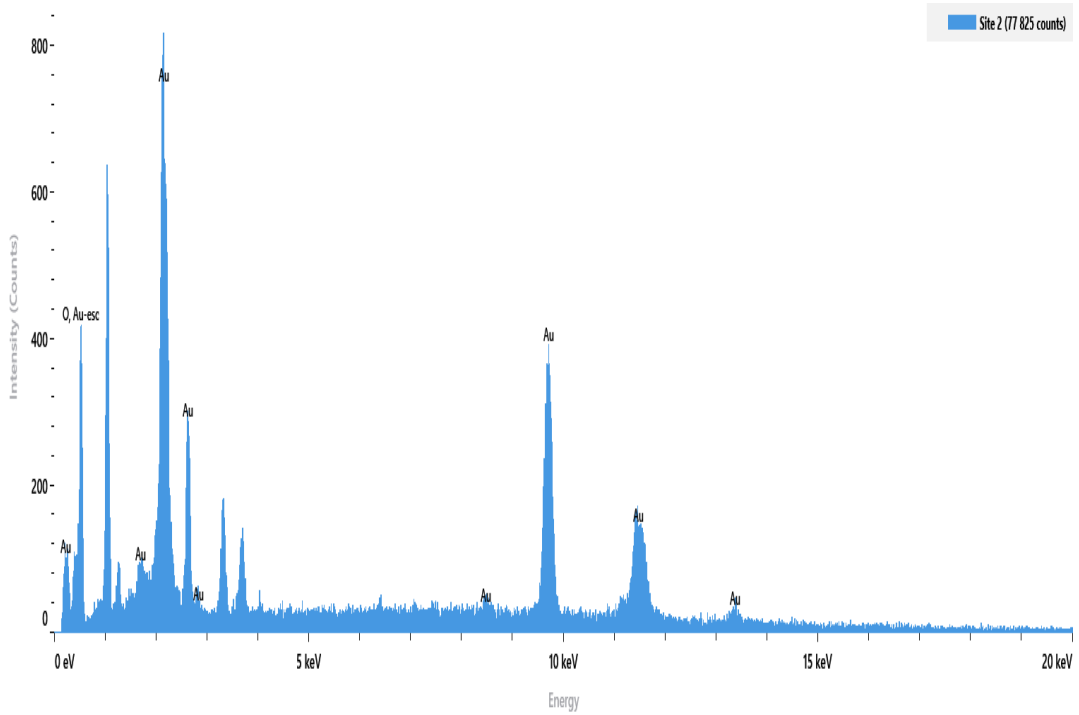

Figure 5: EDX Spectra of AuNPs Powder Extracted from Beetroot Plant

Atomic Force Microscopy (AFM) for Gold Nanoparticles (AuNPs)

Atomic Force Microscopy (AFM) results for gold nanoparticles prepared using beetroot extract provide a precise quantitative characterization of the surface topography at the nanoscale. The average area roughness (Sa) was ≈ 1.93 nm, while the root-squared roughness (Sq) was ≈ 3.89 nm. The maximum height and trough values (Sp ≈ 37.86 nm and Sv ≈ −7.61 nm) showed a total height difference (Sy ≈ 45.47 nm). The linear roughness values (Ra ≈ 0.92 nm and Rq ≈ 1.12 nm) were recorded, with a peak-trough difference (Ry ≈ 4.74 nm) and that can be shown in Figure 6.

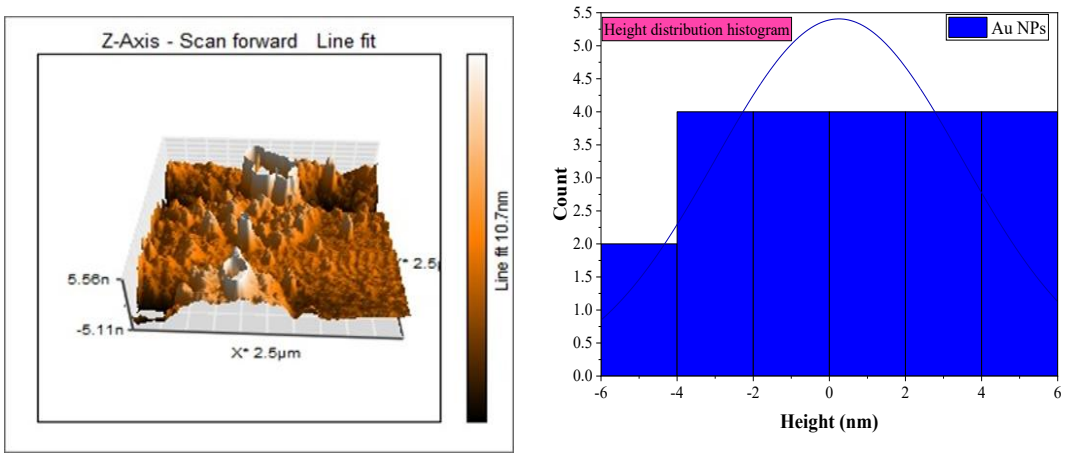

Figure 6: AFM Image and Cumulation Distribution of AuNPs Powder Extracted from Beetroot Plant

Cytotoxicity Test for Gold Nanoparticles (AuNPs)

Six concentrations of gold nanoparticles were tested against two types of cancer cell lines: MDA-MB-231 (triple-negative cancer cell) and MCF-7 (triple-positive cancer cell). The results of the cytotoxicity tests for the gold nanoparticles varied. The highest concentration of gold nanoparticles (2.5 mg/ml) showed 71.03% inhibition against the MDA-MB-231 cells. When the same concentration of gold nanoparticles was tested against the MCF-7 cell line, the inhibition decreased to 29.31%. In addition, the second concentration (1.25 mg/ml) had an inhibitory effect of 49.52% against the MDA-MB-231 cell line and 16.034% against MCF-7 cell line. The remaining concentrations are illustrated in Figure 7.

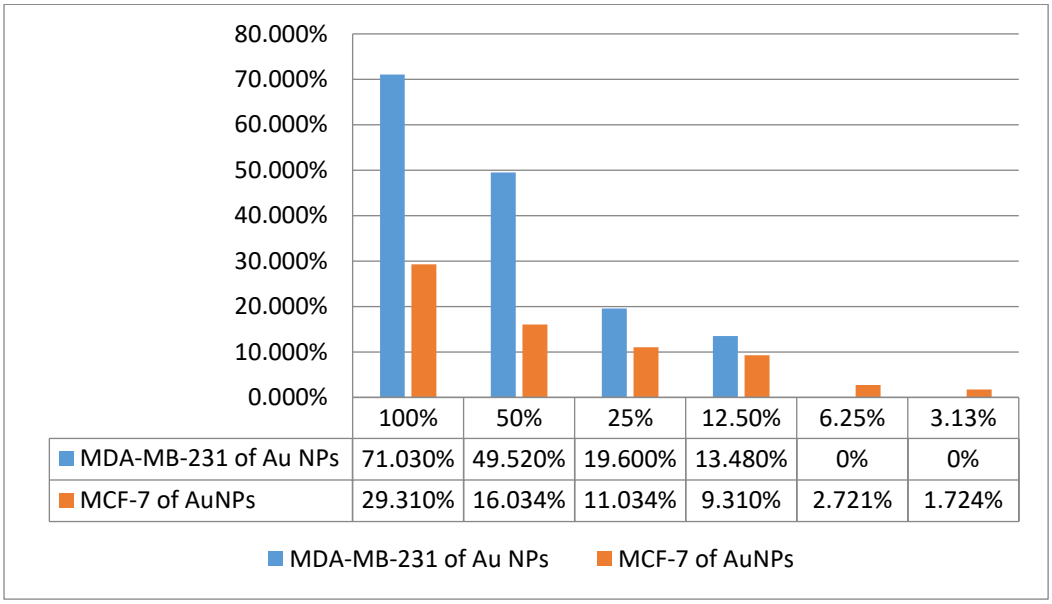

	100%	50%	25%	12.50%	6.25%	3.13%
MDA-MB-231 of Au NPs	71.030%	49.520%	19.600%	13.480%	0%	0%
MCF-7 of AuNPs	29.310%	16.034%	11.034%	9.310%	2.721%	1.724%

Figure 7: Cytotoxicity of AuNPs Against Cancer Cell

DISCUSSION

X-Ray Diffraction (XRD) for Gold Nanoparticles (AuNPs)

The crystalline plane (111), which is the preferred direction for the growth of gold nanoparticles, is shown, as is common in systems prepared by green methods, in addition to the crystalline planes (200), (220), and (311), respectively, confirming the completeness of crystallization and the conformity of the results with the standard data cards for FCC gold (JCPDS No. 04-0784), in agreement with Y. Song and et al [22].

The appearance of small peaks at angles $2\Theta \approx 28°$, 31°, and 34° is attributed to residues of organic compounds and non-reducing salts resulting from the plant extract used. The effects of lattice stresses and surface distortions resulting from the nanoscale may also play a role in the expansion of some peaks and the appearance of low-intensity secondary signals.

It is observed that the high-angle peaks exhibited relatively lower microstress, indicating improved crystal lattice regularity in those crystallographic directions compared to low-angle directions. The variation in crystallographic size and microstress values between different peaks reflects the anisotropic nature of gold nanoparticle growth, in addition to the effect of the green synthesis method, which leads to bio-organic coating on the particle surface. This contributes to increased lattice distortions in some crystal planes, this agreement with G. Albahri et al [23].

Overall, the dominance of the (111) peak and the clarity of the main crystalline peaks confirm the success of the green synthesis method in producing gold nanoparticles with good crystallinity and a relatively regular crystal structure, with expected organic surface effects resulting from the nature of the plant synthesis method.

Ultra Vault – Visible Spectrum (UV-Vis Spectrum) for Gold Nanoparticles (AuNPs)

The increased absorbance in the near-UV region is attributed to the strong absorption of active organic compounds present in the beetroot extract, particularly phenolic compounds and reducing agents, which play a dual role in reducing gold ions and stabilizing the resulting particles.

The appearance of absorbance in the 520–530 nm region without a distinct peak suggests a broad surface plasmon resonance due to the heterogeneous particle size distribution and the possible presence of partial aggregation or strong organic encapsulation on the nanoparticle surface. This behavior dampens the plasmon response and weakens its intensity. Furthermore, the gradual decrease in absorbance with increasing wavelength up to the near-infrared region indicates the stability of the nanoparticles in the liquid medium and the absence of unwanted secondary absorptions, this agreement with S. A. Lee and S. Link [24].

These results confirm that beetroot extract is an effective reducing and stabilizing agent in the preparation of gold nanoparticles in an environmentally friendly manner, and that the optical properties of the formed particles are directly affected by the nature of the biological medium used and by the degree of surface interaction between the nanoparticles and plant organic compounds.

The high EU value is consistent with the broadening and damping of the gold plasmonic resonance response. Increased scattering and surface heterogeneity weaken the sharp plasmonic peak and instead produce a broadened response, gold is a metallic material that does not have a real energy gap, which is agreement with P. Khajegi and H. M. Rashidi [25].

Field Emission-Scanning Electron Microscopy (FE-SEM) for Gold Nanoparticles (AuNPs)

The morphological behavior of the gold nanoparticles is attributed to the dual role of the bioactive compounds present in the beetroot extract. These compounds act as reducing agents for gold ions and as stabilizing agents for the resulting particles. However, strong surface interactions and hydrogen bonds between the organic coatings may lead to particle convergence and partial aggregation. The surface exhibits a distinct roughness and high density of microparticles, indicating a high specific surface area. This morphological structure is expected to align with the UV-Vis absorption spectra, where the heterogeneous size distribution and partial aggregation dampen the surface plasmon resonance of the gold, broadening its spectral response and resulting in a wide shoulder rather than a sharp plasmon peak. Overall, the FE-SEM results confirm the success of the green synthesis method using beetroot extract in producing gold nanoparticles with nanoscale dimensions.

Energy Dispersive X-Ray (EDX) for Gold Nanoparticles (AuNPs)

The EDX results clearly confirm the elemental composition of the formed nanoparticles. (Table 2) The intensity of these peaks compared to the background spectral range indicates a good gold content within the sample, direct evidence of successful bioreduction of gold ions by the active compounds in the plant extract.

The presence of C, and O is attributed to organic residues of the plant extract or salts produced during the preparation process. These bioactive components act as reducing and stabilizing agents (capping agents), preventing excessive growth and clumping of the nanoparticles.

the EDX results, elemental distribution maps, confirm green synthesis method used and confirms the preparation of structurally and chemically stable gold nanoparticles.

Table 2: Elemental compositions weight% and atomic% of AuNPs Powder Extracted from Beetroot Plant

Weight %	Atomic %	Element
23.0	71.7	**O**
7.6	10.7	**Cl**
69.5	17.6	**Au**

Atomic Force Microscopy (AFM) for Gold Nanoparticles (AuNPs)

The surface smear and root-squared roughness data indicate a more uniform nanoscale surface with relatively limited height variation. The height and depth values show distinct nanoprotrusions, representing gold particle deposition or aggregation sites, contrasted with low-lying areas representing interstitial voids or a thin organic layer composed of plant compounds acting as stabilizers.

Furthermore, the linear roughness data indicate relative surface regularity on linear sections, confirming that the gold nanoparticles exhibit a more homogeneous and less agglomerated distribution, consistent with (FE- SEM) images. These results are also consistent with (XRD) data. Functionally, the relatively low surface roughness, combined with the presence of uniform nanoprotrusions, contributes to improved particle stability and enhanced localized electromagnetic field concentration.

Cytotoxicity Test for Gold Nanoparticles (AuNPs)

The variation in the cytotoxicity results of gold nanoparticles against cancer cell lines reveals their ability to inhibit cancer cells. The results also provide a simplified concept for understanding the possibility of using gold nanoparticles in the treatment plan for cancer patients in general and breast cancer patients in particular.

The results indicated a high biological inhibition of gold nanoparticles against the MDA-MB-231 cell line. The ability of gold nanoparticles to inhibit this type of cancer cell can be attributed to genetic mutations in protein 53, which is the protein responsible for repairing damage in the cell , or activate programmed cell death. In addition, this type of cell is more aggressive and has a very high ability to divide, and therefore it spreads rapidly. Therefore, it consumes implanted materials more, which contributes to the entry of nanoparticles into the cell more. Also, the cell membrane of these cells is more permeable due to their constant need for food in order to divide, and therefore they are the most affected by the toxicity of gold nanoparticles, this agreement with L. S. Reinhardt and et al and E. A. Thompson and et al [26][27].

In contrast, MCF-7 cells are less aggressive and divide more slowly. Their protein 53 does not suffer from major genetic mutations that would prevent it from defending the cell and repairing intracellular damage caused by the nanoparticles. Furthermore, due to their limited aggression and slow division, cancer cells may not absorb the same amount of nanoparticles as MDA-MB-231 cells because they do not require the same amount of nutrients, this agreement with K. Kim and et al [28].

Additionally, estrogen and progesterone receptors play a significant role in preventing cancer cell inhibition. MDA-MB-231 cells have abnormalities in their estrogen and progesterone receptors (ER,PR), while MCF-7 cells do not have the same hormone receptor abnormalities.

CONCULSION

This study successfully synthesized gold nanoparticles via a green approach and characterized their morphological, structural, and optical properties. The synthesized nanoparticles exhibited concentration-dependent cytotoxic activity against two breast cancer cell lines MDA-MB-231 cell line and MCF-7 cell line. Gold nanoparticles showed greater cytotoxicity at higher concentrations, whereas at low concentrations, the cytotoxicity was higher against the MCF-7 cell line than against the MDA-MB-231 cell line. These findings highlight the promising potential of green-synthesized nanoparticles for future biomedical applications. However, further studies are required to investigate their mechanisms of action, in vivo efficacy, and safety profiles. This study contributes to ongoing efforts to develop safer and more effective cancer therapies.

ACKNOWLEDGMENT

CONFLICTS OF INTEREST

The author declares that they have no conflicts of interest.

FUNDING

No funding

ETHICS STATEMENTS

REFERENCES

[1] Y. Khan et al., "Classification, Synthetic, and Characterization Approaches to Nanoparticles, and Their Applications in Various Fields of Nanotechnology: A Review," Catalysts, vol. 12, no. 11, Nov. 2022, Art. no. 1386, doi: 10.3390/catal12111386.

[2] A. F. Burlec et al., "Current Overview of Metal Nanoparticles' Synthesis, Characterization, and Biomedical Applications, with a Focus on Silver and Gold Nanoparticles," Pharmaceuticals, vol. 16, no. 10, Oct. 2023, Art. no. 1410, doi: 10.3390/ph16101410.

[3]J. H. Taha, N. K. Abbas, and A. A. F. Al-Attraqchi, "Green synthesis and evaluation of copper oxide nanoparticles using fig leaves and their antifungal and antibacterial activities," International Journal of Drug Delivery Technology, vol. 10, no. 3, pp. 378-382, 2020.

[4] A. I. Osman et al., "Synthesis of green nanoparticles for energy, biomedical, environmental, agricultural, and food applications: A review," Environ. Chem. Lett., vol. 22, pp. 841–887, Jan. 2024. doi: 10.1007/s10311-023-01682-3.

[5] J. H. Taha, "Synthesis, characterization of Ca(OH)_2:TiO_2 nanocomposite and evaluation of its antimicrobial efficacy," Biomedicine, vol. 43, no. 5, pp. 1496-1501, Sep.-Oct. 2023.

[6] I. Sadowska-Bartosz and G. Bartosz, “Biological Properties and Applications of Betalains,” Molecules, vol. 26, no. 9, p. 2520, Apr. 2021. doi: 10.3390/molecules26092520.

[7] T. Nakashima et al., “Spatial and Temporal Variations in Pigment and Species Compositions of Snow Algae on Mt. Tateyama in Toyama Prefecture, Japan,” Front. Plant Sci., vol. 12, p. 689119, Jul. 2021. doi: 10.3389/fpls.2021.689119.

[8] B. Khameneh, M. Iranshahy, V. Soheili, and B. S. F. Bazzaz, “Review on plant antimicrobials: a mechanistic viewpoint,” Antimicrob. Resist. Infect. Control, vol. 8, no. 1, p. 118, 2019. doi: 10.1186/s13756-019-0559-6.

[9] N. P. E. Hikmawanti et al., “The Effect of Ethanol Concentrations as The Extraction Solvent on Antioxidant Activity of Katuk (Sauropus androgynus (L.) Merr.) Leaves Extracts,” in IOP Conf. Ser.: Earth Environ. Sci., vol. 755, no. 1, p. 012060, 2021. doi: 10.1088/1755-1315/755/1/012060.

[10] S. Li, “Morphologies, microstructures and magnetic properties of nanocomposite by hydrothermal methods,” M.E. Thesis, School of Materials Science & Eng., Univ. of New South Wales, Sydney, Australia, 2018. doi: 10.26190/unsworks/3613.

[11] N. Zohora, “Shape controlled biosynthesis of gold nanoprisms using Cinnamomum tamala leaf extract for mercuric ion sensing,” M.S. Thesis, School of Applied Sciences, RMIT Univ., March 2014.

[12] Bai, X., Wang, Y., Song, Z., Feng, Y., Chen, Y., Zhang, D., & Feng, L., “The Basic Properties of Gold Nanoparticles and their Applications in Tumor Diagnosis and Treatment,” International Journal of Molecular Sciences, vol. 21, no. 7, art. 2480, 2020, doi: 10.3390/ijms21072480.

[13] M. Z. Quazi, T. Kim, J. Yang, and N. Park, "Tuning Plasmonic Properties of Gold Nanoparticles by Employing Nanoscale DNA Hydrogel Scaffolds," Biosensors, vol. 13, no. 1, p. 20, Dec. 2022, doi: 10.3390/bios13010020.

[14] N. S. Aminabad, M. Farshbaf, and A. Akbarzadeh, "Recent Advances of Gold Nanoparticles in Biomedical Applications: State of the Art," Cell Biochem. Biophys., vol. 77, no. 1, pp. 1-19, Dec. 2018, doi: 10.1007/s12013-018-0863-4.

[15] A. K. Khan, R. Rashid, G. Murtaza, and A. Zahra, "Gold Nanoparticles: Synthesis and Applications in Drug Delivery," Tropical J. Pharm. Res., vol. 13, no. 7, pp. 1169-1177, Jul. 2014, doi: 10.4314/tjpr.v13i7.23.

[16] M. Das, K. H. Shim, S. S. A. An, and D. K. Yi, "Review on gold nanoparticles and their applications," Toxicol. Environ. Health Sci., vol. 4, no. 4, pp. 189-201, Dec. 2012, doi: 10.1007/s13530-011-0109-y.

[17] H. T. Idriss and J. H. Naismith, "TNF alpha and the TNF Receptor Superfamily: Structure-Function Relationship(s)," Microsc. Res. Tech., vol. 50, no. 3, pp. 184-195, Aug. 2000, doi: 10.1002/1097-0029(20000801)50:3<184::AID-JEMT3>3.0.CO;2-9.

[18] R. Tamilselvi, S. Nandhini, E. Muniyandi, P. Saravanakumar, A. Venkatesh, and V. Prakash, "Cytotoxicity of Metals and Metal Oxides Nanoparticles in Dentistry: A Comprehensive Review," Biomed. & Pharmacol. J., vol. 18, no. 1, pp. 471–481, Mar. 2025. doi: 10.13005/bpj/3101.

[19] M. J. Piao et al., "Silver nanoparticle-induced cell damage via impaired mtROS-JNK/MnSOD signaling pathway," Toxicol. Mech. Methods, vol. 34, no. 7, pp. 803–812, 2024. doi:10.1080/15376516.2024.2350595.

[20] N. P. Nirmal, R. Mereddy, and S. Maqsood, "Recent developments in emerging technologies for beetroot pigment extraction and its food applications," Food Chem., vol. 356, p. 129611, 2021. doi: 10.1016/j.foodchem.2021.129611.

[21] A. S. Abed, Y. H. Khalaf, and A. M. Mohammed, "Green synthesis of gold nanoparticles as an effective opportunity for cancer treatment," Results in Chemistry, vol. 5, p. 100848, Jan. 2023, doi: 10.1016/j.rechem.2023.100848.

[22] Y. Song et al., "Experimental and theoretical study on the synthesis of gold nanoparticles using ceftriaxone as a stabilizing reagent for and its catalysis for dopamine," Gold Bull., vol. 45, no. 3, pp. 153-160, 2012, doi: 10.1007/s13404-012-0060-5.

[23] G. Albahri et al., "Green synthesis of gold nanoparticles using Mandragora autumnalis: characterization and evaluation of its antioxidant and anticancer bioactivities," Pharmaceuticals, vol. 18, no. 9, p. 1294, 2025, doi: 10.3390/ph18091294.

[24] S. A. Lee and S. Link, "Chemical interface damping of surface plasmon resonances," Acc. Chem. Res., vol. 54, no. 8, pp. 1950-1960, 2021, doi: 10.1021/acs.accounts.0c00872.

[25] P. Khajegi and H. M. Rashidi, "Optical properties of gold nanoparticles: shape and size effects," pp. 41-48, 2021, doi: ijop.15.1.41/10.52547.

[26] L. S. Reinhardt, X. Zhang, K. Groen, B. C. Morten, G. N. De Iuliis, A. W. Braithwaite, J.-C. Bourdon, and K. A. Avery-Kiejda, "Alterations in the p53 isoform ratio govern breast cancer cell fate in response to DNA damage," Cell Death Dis., vol. 13, no. 10, p. 907, Oct. 2022, doi: 10.1038/s41419-022-05349-9.

[27] E. A. Thompson, E. Graham, C. M. MacNeill, M. Young, G. Donati, E. M. Wailes, B. T. Jones, and N. H. Levi-Polyachenko, "Differential response of MCF7, MDA-MB-231, and MCF 10A cells to hyperthermia, silver nanoparticles and silver nanoparticle-induced photothermal therapy," Int. J. Hyperthermia, vol. 30, no. 5, pp. 312–323, Aug. 2014, doi: 10.3109/02656736.2014.936051.

[28] K. Kim, H.-r. Cho, and Y. Son, "Astaxanthin induces apoptosis in MCF-7 cells through a p53-dependent pathway," Int. J. Mol. Sci., vol. 25, no. 13, p. 7111, Jun. 2024, doi: 10.3390/ijms25137111.

لتخليق الأخضر وتوصيف جسيمات الذهب النانوية المستخلصة من نبات الشمندر (بيتا فولغاريس) وسميتها الخلوية ضد خلايا سرطان الثدي من نوعي (MDA-MB-231) و(MCF-7)

أبو الفضل يحيى [1]، جنان حسين طه [1]، إبراهيم عبد الله محمود [1]

[1] قسم الفسلجة والفيزياء الطبية، كلية الطب، جامعة النهرين.

الخلاصة

مع زيادة تطبيقات جسيمات الذهب النانوية في علاج السرطان والإيصال الدوائي الطبي، أصبح من الضروري دراسة التأثيرات البيولوجية لهذه الجسيمات. هدفت هذه الدراسة إلى تقييم التأثيرات البيولوجية لجسيمات الذهب النانوية ضد الخلايا السرطانية .تم توصيف جسيمات الذهب النانوية باستخدام عدة تقنيات تحليلية شملت: حيود الأشعة السينية، ومطيافية الأشعة فوق البنفسجية والمرئية، وتشتت الطاقة بالأشعة السينية، ومجهر القوة الذرية، والمجهر الإلكتروني الماسح للانبعاث المجالي. وأكدت نتائج التوصيف النجاح في تخليق جسيمات ذهب نانوية شبه كروية عالية النقاء، وتراوحت أحجام الجسيمات بين 38 إلى 59 نانومتر .تم فحص تأثير السمية الخلوية لجسيمات الذهب النانوية المُخلقة باستخدام مقايسة (إم تي تي) على خطوط خلايا كل من سرطان الثدي نوع (MCF-7) و (MDA-MB-231)بستة تركيزات مختلفة. وأشارت النتائج إلى وجود تأثير تثبيطي لجسيمات الذهب النانوية يعتمد على التركيز ضد كلا خطي الخلايا السرطانية، مع ملاحظة نشاط سمية خلوية عالٍ ضد خط خلايا(MDA-MB-231).

تشير نتائج هذه الدراسة إلى إمكانية استخدام جسيمات الذهب النانوية ضد أنواع مختلفة من خطوط الخلايا السرطانية، وكذلك في علاج الأمراض السرطانية داخل الجسم الحي.

الكلمات المفتاحية: الجسيمات النانوية، جسيمات الذهب النانوية، التخليق الأخضر، الشمندر، سرطان الثدي، السمية الخلوية.